Allosterism in Membrane Binding: A Common Motif of the Annexins?†

Paulo F. F. Almeida,‡ Hitoshi Sohma,§ Katie A. Rasch,|| Catherine M. Wieser,|| and Anne Hinderliter*,||

Department of Chemistry and Biochemistry, University of North Carolina−Wilmington, Wilmington North Carolina 28403, Department of Biomedical Engineering, Sapporo Medical University School of Medicine, Sapporo, 060-8556 Japan, and Department of Pharmaceutical Sciences, North Dakota State University, Fargo, North Dakota 58105

Received March 14, 2005; Revised Manuscript Received June 16, 2005

ABSTRACT: Annexins are a family of proteins generally described as Ca^{2+}-dependent for phospholipid binding. Yet, annexins have a wide variety of binding behaviors and conformational states, some of which are lipid-dependent and Ca^{2+}-independent. We present a model that captures the cation and phospholipid binding behavior of the highly conserved core of the annexins. Experimental data for annexins A4 and A5, which have short N-termini, were globally modeled to gain an understanding of how the lipid-binding affinity of the conserved protein core is modulated. Analysis of the binding behavior was achieved through use of the lanthanide Tb^{3+} as a Ca^{2+} analogue. Binding isotherms were determined experimentally from the quenching of the intrinsic fluorescence of annexins A4 and A5 by Tb^{3+} in the presence or absence of membranes. In the presence of lipid, the affinity of annexin for cation increases, and the binding isotherms change from hyperbolic to weakly sigmoidal. This behavior was modeled by isotherms derived from microscopic binding partition functions. The change from hyperbolic to sigmoidal binding occurs because of an allosteric transition from the annexin solution state to its membrane-associated state. Protein binding to lipid bilayers renders cation binding by annexins cooperative. The two annexin states denote two affinities of the protein for cation, one in the absence and another in the presence of membrane. In the framework of this model, we discuss membrane binding as well as the influence of the N-terminus in modifying the annexin cation-binding affinity by changing the probability of the protein to undergo the postulated two-state transition.

Exactly 40 years ago, Monod, Wyman, and Changeux (MWC)[1] published their landmark paper on the allosteric transitions of proteins (*1*). That work was motivated to a large extent by the goal of describing cooperativity in oxygen binding to hemoglobin. In this report, we use the MWC model in a completely different context, as the simplest model found to describe cooperativity in cation and lipid binding by the annexins. These peripheral membrane proteins are found in abundance in every mammalian cell type (except in erythrocytes) and also in fish, fruit flies, plants, and protozoa, comprising up to 2% of the intracellular proteins (*2*). Annexins consist of a conserved core of four so-called annexin repeats (*3*), where the five amphiphilic α-helices that comprise each repeat assemble into a membrane binding disk, and an N-terminal region, which varies between different annexins. It is the variability in the N-termini that is thought to impart the specificity in the Ca^{2+}- and phospholipid-binding ability of the annexins as well as a variety of phosphorylation sites and binding sites for additional ligands (*3*). Interestingly, annexins do not have any detectable enzymatic activity, intriguing in such a widespread family of proteins. Recent findings implicate a role for annexins in prostate cancer (*4*−*7*), pathogenic infections (*8*), and blood coagulation diseases ("the annexinopathies") such as antiphospholipid syndrome (*9*, *10*).

Although the phospholipid and Ca^{2+} sensitivities vary widely between the annexins, annexin association with membranes has been rationalized primarily on the basis of the hypothesis that annexin function is dependent on Ca^{2+} binding (*2*, *11*). Yet, model studies have shown that annexin binding to membranes is very sensitive to different acidic phospholipids in the bilayer (*2*, *12*). Intracellular localization of annexins varies; removal of their distinct N-termini changes the intracellular distribution of the affected annexin (*13*). In addition, annexins, when bound to the membrane, are able to undergo dramatic conformational changes (*14*, *15*), suggesting a primary role for the membrane in annexin function (*3*).

When annexins bind Ca^{2+} and associate with phospholipid bilayers, Ca^{2+} ions form contacts with the protein and the phospholipids (*16*). This suggests that Ca^{2+} drives annexin binding to the membrane through the formation of a "Ca^{2+} sandwich". Recent work suggested that Ca^{2+} ions bind to

† This work was supported in part by Grants GM64443 (A.H.) and GM59205 (University of Virginia to P.F.F.A.) from the National Institutes of Health. A.H. also acknowledges the donors of the Petroleum Research Fund of the American Chemical Society for partial support of this research.

* To whom correspondence should be addressed. Phone: (701) 231-6556. Fax: (701) 231-8333. E-mail: Anne.Hinderliter@ndsu.edu.

‡ University of North Carolina−Wilmington.

§ Sapporo Medical University School of Medicine.

|| North Dakota State University.

[1] Abbreviations: PS, phosphatidylserine; POPC, 1-palmitoyl-2-oleoyl-*sn*-glycero-3-phosphocholine; POPS, 1-palmitoyl-2-oleoyl-*sn*-glycero-3-phosphoserine; MOPS, 3-morpholinopropanesulfonic acid; LUV, large unilamellar vesicles; K_0, cation-binding affinity of annexin in the absence of lipid; K_1, cation-binding affinity of annexin in the presence of lipid; K_L, lipid-binding affinity of annexin in the absence of cation; X_{PS}, mole fraction of PS; MWC, Monod−Wyman−Changeux.

10.1021/bi050474g CCC: $30.25
Published on Web 07/22/2005

specific helices in annexin A5 and that a highly cooperative network of Ca^{2+}-binding sites is established upon annexin association with the membrane, which can be characterized by a Hill coefficient of approximately 8 (*17*). Annexins also bind Ca^{2+} ions in the absence of phospholipid but with lower affinity (*2*). While this is consistent with a ternary model or a prebinding model in which annexin may not bind phospholipid unless Ca^{2+} is bound first (*18*), additional observations conflict with this model. Annexins with a long N-terminus, such as annexin A2, bind to phospholipid membranes in the absence of Ca^{2+} (*19*). This calls into question both the ternary and prebinding (Ca^{2+}-dependent phospholipid-binding) models; as well, it suggests a role for the N-terminus in modulating the intrinsic phospholipid-binding affinity of the protein core. While each annexin has a distinct binding behavior (*2*), the Ca^{2+}- and phospholipid-binding "core" is very similar between members of the annexin family. A binding model consistent with the wide variety of binding behaviors and also consistent with the similarities in annexin structure seemed lacking. We have approached the association of annexin with the membrane and cations through a rigorous description of the binding process, which makes use of microscopic binding models (*20*, *21*). Binding partition functions were constructed for several microscopic models, and the corresponding binding isotherms were derived from the partition function (*20*). The isotherms were then fit to the experimental data to determine the validity of each specific model. We found that an allosteric model (in the MWC sense) fits annexin A4 and A5 binding data for cation and membrane. In this model annexin binding to the lipid membrane switches its cation binding from a low- to a high-affinity state. The cations bind independently to each annexin state (as in the classic MWC model of allosterism), and the lipid-driven switching between the two states is the source of an apparent cooperativity in cation binding in the presence of lipid. Our allosteric model is in sharp contrast to a highly connected cation-binding affinity driving membrane binding, and we discuss an alternative role in how lipids modulate cation binding and how the N-terminus may modulate the allosteric switching.

EXPERIMENTAL PROCEDURES

Materials. 1-Palmitoyl-2-oleoyl-*sn*-glycero-3-phosphocholine (POPC or 16:0,18:1PC) and 1-palmitoyl-2-oleoyl-*sn*-glycero-3-phosphoserine (POPS or 16:0,18:1PS) were from Avanti Polar Lipids, Inc. (Birmingham, AL). All were greater than 99% pure as determined by thin-layer chromatography (TLC) (*23*, *24*). Potassium chloride was puriss grade, and 3-morpholinopropanesulfonic acid (MOPS) was Biochemika grade from Fluka Chemical Corp. (Ronkonkoma, NY). Chelex-100 ion-exchange resin was from Bio-Rad Laboratories (Rockville Center, NY). Chloroform, methanol, and benzene is HPLC grade (99.5%) from Alfa Aeser (a Johnson Matthey Co., Ward Hill, MA). All other chemicals were of reagent grade.

Preparation of Solutions. Solutions were prepared as in Hinderliter et al. (*23*, *24*). The concentration of $TbCl_3$ stock solutions was checked by titrating new solutions against a standard protein [C2 domains (*24*−*26*)]. The Bradford assay was used to determine protein concentrations.

Expression and Purification of Recombinant Proteins. Purification of wild-type annexins A4 and A5 was based on Ca^{2+}-dependent binding to bovine brain lipids by the method developed in ref *27* with slight modifications (*28*). In brief, expression of protein is induced by isopropyl β-D-thiogalactopyranoside in transformed *Escherichia coli*, and the slurry is harvested by centrifugation, frozen, thawed, mixed with lysozyme, and sonicated. The sonicated mixture was centrifuged and the supernatant collected, incubated with DNase, RNase, and $MgCl_2$, and centrifuged. The collected supernatant was mixed with rat (or bovine) brain lipid membranes and $CaCl_2$. Lipid extraction from rat brain was performed as described (*29*), or brain membrane lipid extracts (Sigma-Aldrich) were used. The pH was adjusted to 7.5, and the mixture was centrifuged; the pellet was resuspended in $CaCl_2$-containing buffer with 150 mM NaCl and centrifuged. The pellet was resuspended in salt-free buffer and centrifuged. Finally, protein (annexin) was extracted with EGTA-containing buffer at pH 7.5 and collected by centrifugation. If necessary, further purification was performed with DEAE-Toyopearl (anion-exchange column). Purified protein was dialyzed against HEPES (pH 7.0) and 100 mM NaCl or appropriate buffer solution overnight, and centrifuged. The protein was frozen in aliquots at −80 °C and used once per titration. The protein was periodically examined for degradation by gel electrophoresis.

Preparation of Large Unilamellar Vesicles (LUV). Lipids were prepared as described before (*23*−*25*).

Fluorescence Spectroscopy Experiments. The binding affinity of the annexins for Tb^{3+} and various lipid mixtures was determined by monitoring changes in energy transfer from the single tryptophan and tyrosines to bound Tb^{3+}. Titrations were also repeated where the single tryptophan was excited and are identical, except somewhat noisier. Advantage was taken of the observation that Tb^{3+} binds to one or more regions of the protein and that this binding is improved in the presence of lipid. Tb^{3+} is a Ca^{2+} analogue, having a similar ionic radius and a higher charge density with the benefit of undergoing fluorescence energy transfer from aromatic amino acids once bound (*30*−*32*). Addition of the lanthanide cation to a protein solution resulted in a decrease in the fluorescence emission maximum of both annexins A4 and A5. The observed fluorescence maximum is in agreement with the observed maximum for annexin A5 under similar conditions, although rat, not human, annexin A5 was used (*33*). This decrease in emission as a function of the cation concentration was normalized to fraction bound, and free ligand was calculated. Fluorescence measurements were made on a Jobin Yvon-Spex Fluorolog-322 with a wavelength set at the excitation maximum of 283 nm, and lamp-corrected emission spectra were recorded. The excitation band-pass was selected after time-trace controls so that photobleaching would be negligible. Double excitation and double emission monochromators had band-passes of 2.0 and 13.5 nm. All samples were stirred continuously in a Teflon-capped 300 μL minifluorometer cell (McCarthy Scientific, Fullerton, CA), and all spectra were collected after a 15 min incubation between additions. Multiple stocks of differing concentrations were used and compared against titrations in which protein had been exhaustively dialyzed. Results did not vary with stock solutions.

Titrations of Annexins with Tb^{3+} and Lipid. Titration data were gathered by following the quenching of the intrinsic fluorescence of annexins A4 and A5 by the lanthanide Tb^{3+}.

Excitation of the lanthanide was achieved indirectly through chelation by the protein and fluorescence energy transfer from directly excited aromatic amino acids within the protein to the lanthanide (*32*). The fluorescence energy transfer from the protein to the lanthanide was detected as quenching of the intrinsic protein fluorescence. The loss of fluorescence was normalized and expressed as fraction bound. The titration curves were corrected for light scattering, which is significant at the higher lipid concentrations in the lipid titration data, or for a slight drift that occurs at high cation concentrations in a few of the Tb^{3+} titration data for annexin A5, by subtracting a linear ramp determined from the high concentration regime. The added total ligand was corrected to free ligand for each corresponding fractional bound value, after accounting for maximum numbers of ligands bound at saturation to the protein. Experimental data were corrected for free ligand versus fraction bound per site on the protein. Total ligand was corrected for free ligand by calculating the fraction bound to protein and subtracting bound from total ligand added. As a fluorescence change is not detectable upon addition of membrane vesicle alone, lipid titration data were gathered by titrating lipid into a solution of protein and a subsaturating concentration of terbium ion. Addition of lipid increased the affinity of protein for Tb^{3+}, detectable as a loss of protein fluorescence upon cation binding. Annexin A4 and A5 data were corrected assuming that the surface of the membrane covered by a protein corresponds to 10 lipids. This is approximately the number of lipids that fits under an annexin molecule (*34*).

Binding Isotherms. Binding isotherms were derived from the binding partition function (*20*). Briefly, the binding partition function contains a term proportional to the probability of observing each state of the protein. In our model there are two fundamental states of annexin: (1) free in aqueous solution, with (a variable number of) bound Tb^{3+} ions in aqueous solution, and (2) bound to a lipid vesicle, with (a variable number of) bound Tb^{3+} ions. Equation 1 (see Results) then gives the binding partition function for this system. To obtain the binding isotherms from the partition function, the following derivative is calculated, $\theta = (1/N)(x/Q)\, dQ/dx$, where $x =$ [Tb] or [L] and $N = n$ for Tb^{3+} (n is maximum number of Tb^{3+} sites on the protein) and $N = 1$ for lipid titrations (one protein is either bound to the one lipid vesicle or not); θ is the fractional saturation of Tb^{3+} sites on the annexin or the fraction of proteins bound to the lipid. The resulting binding isotherms are given by eq 2 for Tb^{3+} binding and eq 3 for lipid binding. Equations 2 and 3 were used to analyze the experimental binding isotherms. A global fit of these equations to all of the corresponding data (Tb^{3+} and lipid titrations simultaneously) for each annexin (A4 and A5) was obtained using the Simplex algorithm (*35*).

RESULTS

We have sought to understand the binding of annexins to lipid membranes and how it is influenced by binding of Ca^{2+}, which was mimicked by Tb^{3+} in our experiments, to these proteins. In the presence of lipid, the Tb^{3+} binding isotherm suggests greater cation-binding cooperativity and affinity (Figure 1) in comparison with a titration in the absence of lipid (Figure 2). Titration data that exhibit apparent cooperativity are often fit by the Hill equation (*36*), and an initial

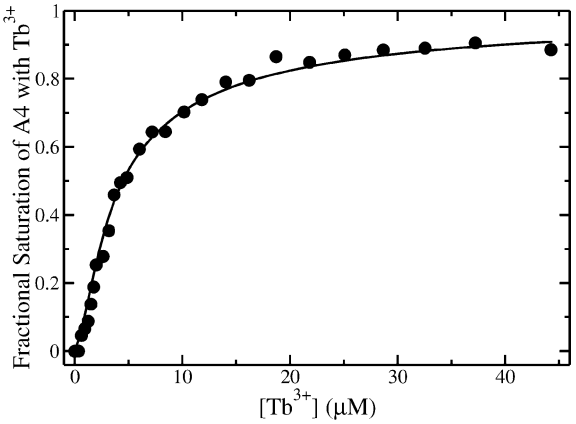

FIGURE 1: Binding of Tb^{3+} to annexin A4 in the presence of 300 μM POPC/POPS (90:10). The signal arising from quenching of the intrinsic protein fluorescence was used. The loss of fluorescence was normalized and expressed as fraction bound. The added total ligand was corrected to free ligand, taking into account the total number of ligands occupying the protein at saturation and the concentration of protein (0.27 μM). Data were corrected for six cation-binding sites. All titrations were carried out in decalcified 2 mM MOPS and 100 mM KCl, pH 7.5. The line is eq 2 with the parameters that gave the best global fit of eqs 2−4 to all annexin A4 data simultaneously. The global fit parameters are given in the text.

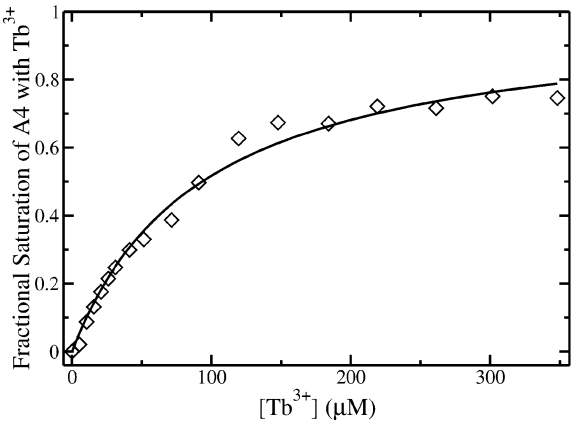

FIGURE 2: Binding of Tb^{3+} to annexin A4 in the absence of lipid. Details are the same as in Figure 1. The line is eq 2 with the parameters that gave the best global fit of eqs 2−4 to all annexin A4 data simultaneously. The cation-binding affinity obtained is $K_0 = 1.07 \times 10^4\ M^{-1}$.

fit to this set of data appeared consistent with that approach. However, the Hill equation suffers from the disadvantage that it is not based on a microscopic binding model. In addition, as an empirical relationship, it does not provide further insight into how annexin Tb^{3+} binding influences its lipid-binding properties. Therefore, binding partition functions were derived for several microscopic models and tested through fitting of the binding isotherms generated from them to experimental titration data. The approach to binding isotherms through the use of microscopic binding partition functions provides a much more in-depth understanding of the association process as the probabilities of each protein state can be directly and simply obtained from the partition function (*20*).

We have found that an allosteric model, in the Monod−Wyman−Changeux (MWC) sense for hemoglobin (*1*, *21*), is consistent with the experimental binding data. In the MWC

model of oxygen binding by hemoglobin, the protein exists in two states, T and R. Oxygen molecules bind to *each state* independently of each other and with identical microscopic association constants to each of the four sites in the protein. The cooperativity occurs because of a transition from the T to R state, which is made more probable as the number of oxygen molecules bound to the T state increases. Monod et al. (*1*) called this an *allosteric transition* (this meaning of *allosteric* should be distinguished from an allosteric activator or inhibitor, which means that the effector binds to a site other than the active site on an enzyme). Similarly, we consider that annexins exist in two states, one in aqueous solution and one bound to the lipid membrane. Each state can bind cations (Ca^{2+} or Tb^{3+}) at n sites on the protein; those sites are assumed to be identical in their cation-binding strength. (Although there is some independent experimental evidence suggesting that the annexin Ca^{2+}-binding sites are *not* identical in their cation affinity, we made this simplifying assumption here because we found no significant improvement in the fits by allowing for sites with different binding affinities.) Apparent weak cooperativity in cation binding (Figure 1) does result because when the protein is bound to lipid, its cation-binding affinity increases. Therefore, because of thermodynamic coupling between lipid and Tb^{3+} binding by the annexin, as the protein, initially in solution, begins to bind Tb^{3+}, its lipid affinity increases, which in turn leads to increased affinity for Tb^{3+}.

The model proposed here is the simplest possible for this system. In the absence of lipid, Tb^{3+} binding by annexins is hyperbolic (not cooperative) (Figure 2). This means that Tb^{3+} titration data can always be described by a partition function of the form $q_0 = (1 + K_0[Tb^{3+}])^n$, where K_0 is the binding constant for Tb^{3+}. The maximum number of binding sites, n, has no influence on the shape of the binding isotherm, $(1/n)(d \ln(q_0))/d \ln([Tb^{3+}])$, and cannot be determined from a single set of these titration data. To describe binding in the presence of lipid, the simplest possibility is to use a similar function but with a binding constant for Tb^{3+}, K_1, that is not necessarily identical to K_0, $q_1 = (1 + K_1[Tb^{3+}])^n$. For the entire system, including binding of Tb^{3+} to the protein and binding of the protein to the lipid membrane, the simplest possibility for the partition function (Q) is just a combination of q_0, q_1, and a factor describing binding to the lipid ($K_L[L]$); that is

$$Q = (1 + K_0[Tb])^n + K_L[L](1 + K_1[Tb])^n \qquad (1)$$

In this equation, [L] is the lipid vesicle concentration (expressed in this work in terms of lipid concentration in the outer leaflet of the lipid vesicles), [Tb] is Tb^{3+} concentration, K_L is the lipid-binding constant in the absence of Tb^{3+}, and n is the maximum number of Tb^{3+} ions that can be bound per annexin. The binding of Tb^{3+} to each annexin state (lipid-associated or in aqueous solution) is assumed to be independent of the number of Tb^{3+} already bound. That is, within each annexin state, the Tb^{3+} ions are considered independent and identical ligands. In eq 1, the first term is proportional to the probability of annexin in aqueous solution, with 1 to n Tb^{3+} ions bound, and the second term is proportional to the probability of annexin being associated with the lipid membrane, with 1 to n Tb^{3+} ions bound. The binding isotherms for Tb^{3+} and lipid, obtained from the partition function of eq 1 as described in Experimental Procedures, are then for Tb^{3+} binding

$$\theta_{Tb} = (K_0[Tb](1 + K_0[Tb])^{n-1} + K_L[L]K_1[Tb](1 + K_1[Tb])^{n-1})/Q \qquad (2)$$

and for lipid binding

$$\theta_L = (K_L[L](1 + K_1[Tb])^n)/Q \qquad (3)$$

In addition, the lipid affinity in the absence of cation, K_L, depends on the mole fraction (X_{PS}) of phosphatidylserine (PS) present in the lipid vesicles. We have found that this dependence can be well described by

$$K_L = A_0 \exp(K_{PS}X_{PS}) \qquad (4)$$

where A_0 is the binding constant to pure phosphatidylcholine vesicles (PC) in the absence of cation ($X_{PS} = 0$) and K_{PS} is a constant describing the dependence on PS content.

We have found that this simple model is able to describe binding of Tb^{3+} and lipid to both annexins A4 and A5. More complicated models, which might include the selective change in Tb^{3+}-binding affinity to a subset of sites on annexin upon binding of the protein to a lipid membrane, are of course possible and will certainly be able to fit the data. However, they are not justified by the present data. The model proposed here is allosteric in the MWC sense, in that there are two states of the annexin (in solution and membrane-bound) and that cation binding to the protein brings about a transition between the two states. The model does *not* imply that there is a conformational change in the annexin, though it is consistent with such a change. It suggests that annexins have the plasticity of adopting more than one state, which may be important for their function, as discussed below. These are the general features of the model. While it fits both annexins A4 and A5, the specifics of lipid and Tb^{3+} binding to each annexin are different.

Cation and Lipid Binding by Annexin A4. The X-ray structures of bovine annexin A4 show at most 2 Ca^{2+} ions bound (*37*, *38*). However, those same X-ray structures reveal 12 potential cation-binding sites. Therefore, we have sought to determine this number (n) independently. First, we examined Tb^{3+} binding under almost irreversible conditions by performing the Tb^{3+} titrations in the presence of a large concentration of lipid (0.5−1 mM) vesicles with a high content of PS (40 mol %). Under these conditions, a break in the intrinsic protein fluorescence upon Tb^{3+} binding is observed, which is an indication of the stoichiometric ratio of Tb^{3+}/A4 (Figure 3A). However, these measurements have a significant uncertainty associated with them, mainly because of light scattering increase from the high lipid concentrations, so that we found $n = 5-9$ Tb^{3+} sites on annexin A4 in different experiments. Further improvement on the determination of n was obtained from the evaluation of the χ^2 for global fits to all A4 binding data to both Tb^{3+} and lipid (Figure 3B). This indicated that a number of cation-binding sites, $n = 6$, gives the best results, and this value was used in the analysis. It should be noted that other values for n from 4 to 9 lead to results that do not differ qualitatively from those obtained with $n = 6$. Therefore, this number does not have a significant impact of the overall analysis and

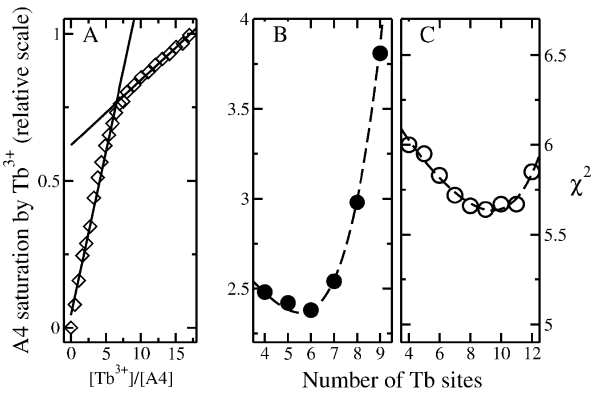

FIGURE 3: (A) Titration of annexin A4 with $TbCl_3$ under quasi-irreversible cation-binding conditions. The change in protein fluorescence as a function of $TbCl_3$ concentration was monitored in the presence of a high concentration of POPC/POPS lipid vesicles (0.5 mM) with a high PS content (40%) to increase, as much as possible, the binding affinity of the cation for the protein. The break in this curve occurs at 6.5 Tb^{3+}/A4 ratio, suggesting that this is the approximate number of binding sites available on the protein. (B) Plot of the dependence of the quality of the global fit, as measured by the χ^2 value, on the maximum number of binding sites in annexin A4. A value of $n = 6$ appears to correspond to the minimum in χ^2. (C) χ^2 plot for annexin A5. The scale is the same as for the A4 plot, showing that the dependence on the number of cation-binding sites is shallower. In any case, the best global fits appear to be obtained with $n = 9$.

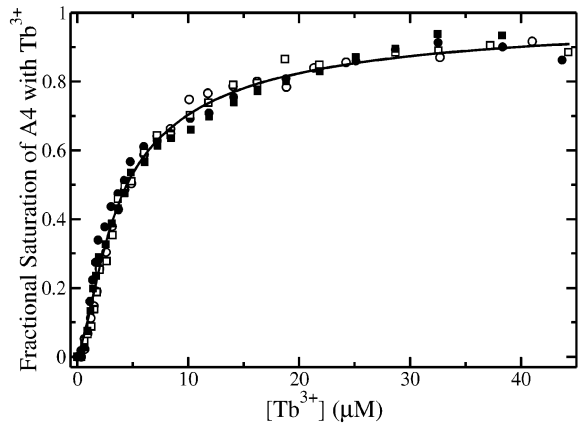

FIGURE 4: Binding of Tb^{3+} to annexin A4 in the presence of POPC/POPS lipid vesicles with varying PS content. Tb^{3+} titrations were carried out in the presence of a constant concentration of 15 μM PS in the outer leaflet of the LUV. To achieve a constant PS concentration in the cation titrations, total lipid varied with lipid composition; titrations in the presence of POPC/POPS (80:20), POPC/POPS (85:15), POPC/POPS (90:10), and POPC/POPS (95:5) had total lipid concentrations of 150, 200, 300, and 600 μM, respectively. Data were corrected for six cation-binding sites. The line is eq 2 with the parameters that gave the best global fit of eqs 2−4 to all annexin A4 data simultaneously. Only one line is shown for all titrations because they are essentially superimposable, indicating that the critical factor is the total PS concentration present. Symbols are as follows: PC/PS (95:5) (solid squares), PC/PS (90:10) (open squares), PC/PS (85:15) (solid circles), and PC/PS (80:20) (open circles).

conclusions. The titration of annexin A4 with $TbCl_3$ in the absence of lipid yields a hyperbolic binding isotherm (Figure 2) with a site binding constant for cation, $K_0 = 1.07 \times 10^4$ M^{-1}. In the presence of lipid, the affinity of annexin A4 for Tb^{3+} increases significantly, as shown in Figure 4, where titrations of annexin A4 with Tb^{3+} are represented. A model with identical and independent discrete binding sites (eq 2, with $n = 6$) fits the data globally very well (Figure 4). Titrations of annexin A4 with POPC/POPS lipid vesicles with varying PS content ($X_{PS} = 0-0.20$) were also performed, and the data were fitted with eq 3 (Figure 5). The global fit of eqs 2−4 to the A4 data, which includes both sets of titrations (Figures 2, 4, and 5), yielded the following best parameter values: $K_0 = 1.07 \times 10^4$ M^{-1}, $K_1 = 2.46 \times 10^5$ M^{-1}, $A_0 = 1.2 \times 10^3$ M^{-1}, and $K_{PS} = 7.15$. For easy reference, the corresponding dissociation constants are $1/K_0 = 94$ μM, $1/K_1 = 4$ μM, and $1/A_0$ (dissociation constant for pure PC) = 830 μM. Thus, we find that $K_1 \gg K_0$; that is, the affinity for Tb^{3+} is much larger when annexin A4 is in the membrane-bound state, though this was not an a priori imposed condition. The transition from one annexin state to the other appears as positive cooperativity toward cation binding. The binding affinity for lipid in the *absence* of cation, K_L, which varies with the mole fraction of PS (X_{PS}) is then obtained from eq 4 and found to be of the order of 10^3 M^{-1} for all PS/PC mixtures examined ($X_{PS} = 0-0.20$). Dissociation constants for annexin A4 for PS in the absence of cation then vary for $X_{PS} = 0.05$, 0.10, 0.15, and 0.20 as $1/K_L = 580$, 410, 290, and 200 μM, respectively (Figure 8).

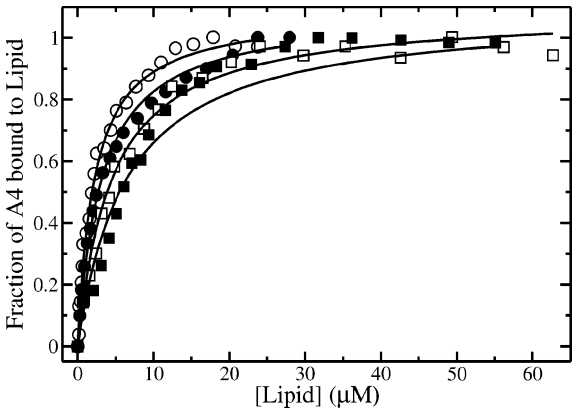

FIGURE 5: Binding of annexin A4 to lipid in the presence of a subsaturating Tb^{3+} concentration (5 μM). The *X*-axis is the free lipid concentration present in the outer leaflet of the lipid bilayer of the vesicles. Lipid was titrated into a solution of protein and a fixed concentration of cation. The data were corrected assuming that the surface of the membrane covered by protein corresponds to 10 lipids. Symbols are as follows: POPC/POPS (95:5) (solid squares), POPC/POPS (90:10) (open squares), POPC/POPS (81:15) (solid circles), and POPC/POPS (80:20) (open circles). The lines represent eq 3 with the parameters that gave the best global fit of eqs 2−4 to all annexin A4 data simultaneously.

Cation and Lipid Binding by Annexin A5. The same two-state or allosteric model correctly describes binding of Tb^{3+} and lipid to annexin A5. The X-ray structure of rat annexin A5 (*15*), which is the specific annexin A5 we used, shows seven occupied cation-binding sites. However, this number has a considerable uncertainty; other published structures of annexins A5 have between 2 and 9 Ca^{2+} ions bound: 2 (*39*), 3 (*40*), 4 (*41*, *42*), 5 (*43*, *44*), 7 (*15*), and 9 (*22*). Therefore, we have attempted to narrow the range of maximum number of binding sites using the same approach employed for A4. The measurements of Tb^{3+} binding by fluorescence spectroscopy under irreversible conditions did not work as well for A5 due in part to weaker membrane coupling to cation binding. However, a plot of the χ^2 for global fits to all A5 binding data (Figure 3C) indicated that a number of cation-binding sites, $n = 9$, gives the best results, and this value

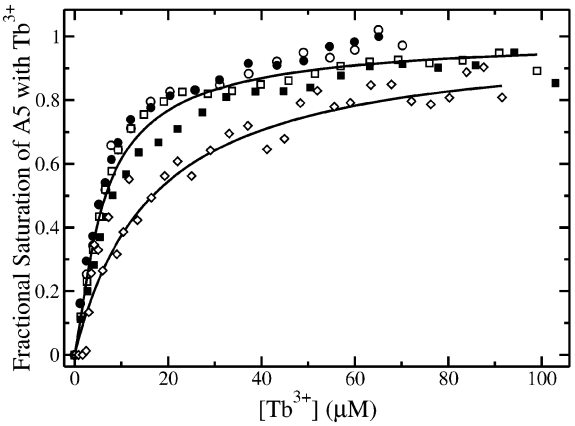

FIGURE 6: Binding of Tb^{3+} to annexin A5 in the presence and absence of lipid. The signal arising from quenching of the intrinsic protein fluorescence was used. The loss of fluorescence was normalized and expressed as fraction bound. The added total ligand was corrected to free ligand, taking into account the total number of ligands occupying the protein at saturation and the concentration of protein. Data were corrected for nine cation-binding sites. All titrations were carried out in decalcified 2 mM MOPS and 100 mM KCl, pH 7.5. Cation titrations were carried out in the presence of a constant concentration of 15 μM PS^- found on the outer leaflet of the LUV. To achieve a constant PS concentration in all titrations, total lipid varied with lipid composition; titrations in the presence of POPC/POPS (60:40), POPC/POPS (70:30), POPC/POPS (80:20), and POPC/POPS (90:10) had total lipid concentrations of 75, 100, 150, and 300 μM, respectively. The lines represent eq 2 with the parameters that gave the best global fit of eqs 2−4 to all annexin A5 data simultaneously. Only one line is shown for all titrations in the presence of lipid because they all are essentially superimposable. Symbols are as follows: no lipid present (diamonds), with PC/PS (60:40) (open circles), with PC/PS (70:30) (solid circles), with PC/PS (80:20) (open squares), and with PC/PS (90:10) (solid squares).

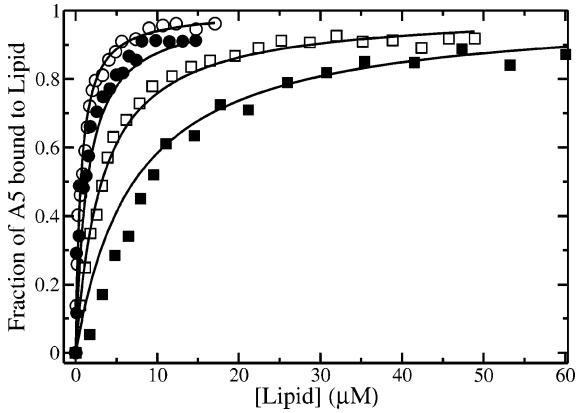

FIGURE 7: Binding of annexin A5 to lipid in the presence of a subsaturating Tb^{3+} concentration (10 μM). The *X*-axis is the free lipid concentration present in the outer leaflet of the lipid bilayer of the vesicles. Lipid was titrated into a solution of protein and a fixed concentration of cation. The data were corrected assuming that the surface of the membrane covered by protein corresponds to 10 lipids. The lines represent eq 3 with the parameters that gave the best global fit of eqs 2−4 to all annexin A5 data simultaneously. Symbols are as follows: POPC/POPS (60:40) (open circles), POPC/POPS (70:30) (solid circles), POPC/POPS (80:20) (open squares), and POPC/POPS (90:10) (solid squares).

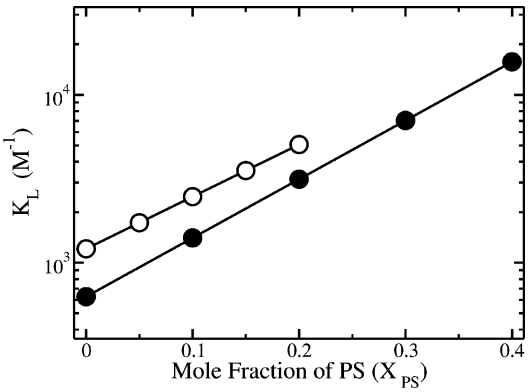

FIGURE 8: Dependence of the lipid-binding constant of annexins A4 (open circles) and A5 (closed circles) on the mole fraction of PS (X_{PS}) in the vesicles. The values were calculated from eq 4 using the parameters obtained from the fits of eqs 2−4 to the experimental data for each of the annexins. The points are shown to indicate the specific lipid mixtures studied for each annexin.

was used in the analysis. It should be noted that other values for *n*, especially from 6 to 11, lead to results that do not differ significantly from those obtained with $n = 9$. In any case, as with A4 the exact number does not have a significant impact of the overall analysis and conclusions. As with annexin A4, binding of cation alone by annexin A5 yields a hyperbolic isotherm. The Tb^{3+} binding isotherms in the absence of lipid and in the presence of several mixtures of POPC/POPS are shown in Figure 6. In the presence of lipid, the binding isotherm reveals an increased affinity for Tb^{3+} and an apparent cooperativity in Tb^{3+} binding, but the effect of lipid is much weaker than with A4. The experimental cation-binding data were fit with eq 2. It is evident that all isotherms in the presence of lipid are well described by the same equation (Figure 6). The binding isotherms corresponding to the titrations of annexin A5 with POPC/POPS lipid vesicles in the presence of Tb^{3+} are shown in Figure 7. The lines shown are the corresponding fits of eq 3 to the experimental data. The binding of annexin A5 to lipid is also very dependent on the PS content of the vesicles. The global best fit to all annexin A5 Tb^{3+}- and lipid-binding data simultaneously yielded the following parameter values: $K_0 = 6.0 \times 10^4$ M^{-1}, $K_1 = 1.7 \times 10^5$ M^{-1}, $A_0 = 6.3 \times 10^2$ M^{-1}, and $K_{PS} = 8.05$. For ease of comparison, the analogous dissociation constants are $1/K_0 = 17$ μM, $1/K_1 = 6$ μM, and $1/A_0$ (or dissociation constant for pure PC) = 1600 μM. Similar to annexin A4, in the *absence* of cation, the annexin−lipid association constant, K_L (calculated from eq 4), is of the order of 10^3 M^{-1} for PS/PC mixtures containing up to 20% PS but increases to 10^4 M^{-1} for 40% PS (Figure 8). Dissociation constants for annexin A5 for PS in the absence of cation then vary for $X_{PS} = 0.10$, 0.20, 0.30, and 0.40 as $1/K_L$ = 1400, 320, 140, and 63 μM, respectively. In comparison with annexin A4, A5 binds Tb^{3+} better in solution: the dissociation constants for the cation are approximately 100 μM for A4 and 17 μM for A5.

DISCUSSION

Let us briefly summarize lipid and Tb^{3+} binding by annexins A4 and A5. In the presence of lipid, the affinity of annexin for cation increases and the binding isotherms change from hyperbolic to weakly sigmoidal. In the model proposed, this occurs because of an allosteric transition from the annexin solution state to its membrane-associated state. Thus, the apparent cooperativity in cation binding does not result from enhancement of cation affinity by previous cation binding but from a thermodynamic coupling between lipid

and Tb^{3+} binding. It may be pointed out that the isotherms for lipid binding are still hyperbolic, as they should be. This is because the ligand is in fact the lipid vesicle, and binding of a vesicle to one annexin molecule does not increase the tendency of a second lipid vesicle to bind to it or of other annexins to associate with that lipid vesicle. It is possible that cooperativity in binding individual PS molecules within the membrane to the annexin occurs when annexin binds cation. However, we did not treat PS binding to annexin as association with individual PS-binding sites (as for Tb^{3+}); rather, the effect of PS on annexin binding to lipid vesicles was modeled as a smeared attraction, which could be electrostatic in origin. The use of a discrete site-binding model for PS association with annexin (*45*, *46*) was tried and gave similar results. Because our model is simpler, has fewer parameters, and produced comparable fits, we decided to remain with this simpler version. The fact that a global fit to all data for each annexin tested is able to describe the experimental binding curves very well and that the same model, with slightly different parameters, is able to describe the data for both annexins A4 and A5 lends strong support to the hypothesis that a two-state model is adequate to describe annexin interactions with its most common ligands (lipid and cations). The relation between the two states defined here (membrane-associated and in solution) and possible different conformational states of the annexins is not established by our data. However, it appears to be a very plausible and attractive hypothesis.

With PS as a minor component, the membrane-binding affinity (K_L) of annexins A4 and A5 is so small that the probability of membrane association is low. K_L, as calculated from our model in the absence of cation, varies exponentially with the mole fraction of PS, X_{PS} (Figure 8). Annexins A4 and A5 were chosen for this study because they have short N-termini. This fact, in combination with the result that the same allosteric binding model describes lipid- and Tb^{3+}-binding data for both annexins, suggests that our model captures the essence of the membrane-binding behavior of the annexin core. Furthermore, the results indicate that the membrane-binding core of the annexins is very sensitive to PS content. Annexins with complex N-termini, such as annexins A1 and A2, exhibit higher lipid-binding affinity (*2*, *19*, *47*) than annexins A4 and A5. Annexin A2 may also undergo Ca^{2+}-independent membrane binding. An interpretation of this observation is that the intrinsic lipid-binding affinity of the protein core may be influenced by the N-terminus. Therefore, it appears that, in the annexins, the lipid affinity of the protein core is modified by both cation and the N-terminus. If the core lipid-binding affinity were high, sensitive modification of the lipid-binding affinity by cation-binding sites within the protein core or the N-terminus would not be possible. The protein would always be bound.

The N-terminus, although located opposite to the membrane-binding face, influences the lipid-binding affinity of annexins (*3*). In annexin A1, the N-terminus forms an α-helix and has numerous contacts with the protein core. Upon addition of Ca^{2+}, the helix is exposed and becomes available for interactions with additional ligands or with the membrane (*48*). The N-terminus of annexin A3 inserts into the center of the protein where the four annexin repeats hinge together (*49*). The tryptophan residue in the N-terminus of annexin A3 was found to have specific interactions with the core of the protein that modulated its membrane binding, as indicated by lipid cosedimentation experiments (*49*). Urea denaturation studies reveal an unfolding of the N-terminus separate from the core of the protein (*50*), and the authors note that this provides important insights into the role of the N-termini tryptophan-core contact in the overall conformational flexibility of annexin A3. Furthermore, examination of several homologous annexins A5 indicates that even the short N-terminus stabilizes the overall structure in solution (*51*). Previous work using fluorescence spectroscopy (*52*) had already suggested that N-termini-truncated mutants in solution exhibit a more relaxed conformation. This flexibility of the annexins is probably a consequence of an abnormally low hydrophobicity of the protein inner core, which is indicated by the small denaturation heat capacity changes of the annexins (*53*, *54*).

The interaction of the protein core with either the N-terminus or the membrane would then essentially "quench" the structural fluctuations; with the more rigidified structure thus acquired, the annexins would bind cation with greater affinity. If the binding of cation requires an ordering of the protein close to the binding sites, this would correspond to an entropy penalty upon cation binding, which would consequently reduce cation affinity. However, this entropy penalty would already have been paid for if the binding to the membrane or interaction with the N-terminus would have "frozen" the protein conformation in its more ordered state, with a high cation affinity. Within our allosteric model, quenching of the fluctuations upon membrane association corresponds to the shifting of the protein to the higher cation-affinity state. The finding of greater cation and membrane affinity of annexins with long N-termini (*3*, *19*) suggests that interaction of the N-terminus with the core can also shift the annexin to the higher cation-affinity state. In the framework of our model, we now suggest that their N-termini modify the annexin cation-binding affinity by changing the probability of the protein to undergo the postulated two-state transition. Mutations of residues in the N-terminus and within the Ca^{2+}-binding sites may then change the probability of the protein to switch from one state to the other (*17*). As these mutations may change the ability of the annexin to undergo the two-state transition, an overall change of cation affinity would be observed.

An allosteric model such as used here is often interpreted as due to a conformational change in the protein. Although a conformational change is not required, it may occur, and it may be locally subtle and spread out globally. The recent work of Isas et al. (*55*) on the nonmammalian annexin B12 shows a rigidification of the lipid-contacting loops of the protein upon membrane association in the presence Ca^{2+}. Such a rigidification would be consistent with our allosteric model if the two states we propose corresponded to distinct physical states of the protein. Even more extreme is the observation that, at low pH, annexin B12 inserts into the lipid bilayer, at least partially (*14*, *15*, *55*). These examples may thus reflect the special capacity of the annexins to undergo global structural transitions (while conserving secondary structure), consistent with an allosteric model.

ACKNOWLEDGMENT

P.F.F.A. and A.H. thank Rod Biltonen for support and teaching over many years of collaboration. We thank Carl

Creutz for critical reading of the manuscript and acknowledge Gary Stoop and Ernie McCoy at Jobin Yvon-Spex for all of their help.

REFERENCES

1. Monod, J., Wyman, J., and Changeux, J.-P. (1965) On the nature of allosteric transitions: a plausible model, *J. Mol. Biol. 12*, 88−118.
2. Raynal, P., and Pollard, H. B. (1994) Annexins: the problem of assessing the biological role for a gene family of multifunctional calcium- and phospholipid-binding proteins, *Biochim. Biophys. Acta 1197*, 63−93.
3. Gerke, V., and Moss, S. E. (2002) Annexins: from structure and function, *Physiol. Rev. 82*, 331−371.
4. Xin, W., Rhodes, D. R., Ingold, C., Chinnaiyan, A. M., and Rubin, M. A. (2003) Dysregulation of the annexin protein family is associated with prostate cancer progression, *Am. J. Pathol. 162*, 255−261.
5. Kang, J. S., Calvo, B. F., Maygarden, S. J., Caskey, L. S., Mohler, J. L., and Ornstein, D. K. (2002) Dysregulation of annexin I protein expression in high-grade prostatic intraepithelial neoplasia and prostate cancer, *Clin. Cancer Res. 8*, 117−123.
6. Srivastava, M., Bubendork, L., Srikantan, V., Fossom, L., Nolan, L., Glasman, M., Leighton, X., Fehrle, W., Pittaluga, S., Raffeld, M., Koivisto, P., Willi, N., Gasser, T. C., Kononen, J., Sauter, G., Kallioniemi, O. P., Srivastava, S., and Pollard, H. B. (2001) ANX7, a candidate tumor suppressor gene for prostate cancer, *Proc. Natl. Acad. Sci. U.S.A. 98*, 4575−4580.
7. Chetcuti, A., Margan, S. M., Russell, P., Mann, S., Miller, D. S., Clark, S. J., Rogers, J., Handelsman, D. J., and Dong, Q. (2001) Loss of annexin II heavy and light chains in prostate cancer and its precursors, *Cancer Res. 61*, 6331−6334.
8. Zobiack, N., Rescher, U., Laarmann, S., Michgehl, S., Schmidt, M. A., and Gerke, V. (2002) Cell-surface attachment of pedestal-forming enteropathogenic *E. coli* induces clustering of raft components and a recruitment of annexin 2, *J. Cell Sci. 115*, 91−98.
9. Rand, J. H. (2000) Antiphospholipid antibody-mediated disruption of the annexin-V antithrombotic shield: a thrombogenic mechanism for the antiphospholipid syndrome, *J. Autoimmun. 15*, 107−111.
10. Rand, J. H. (1999) Annexinopathies, *N. Engl. J. Med. 340*, 1035−1036.
11. Swairjo, M. A., and Seaton, B. A. (1994) Annexin structure and membrane interactions: a molecular perspective, *Annu. Rev. Biophys. Biomol. Struct. 23*, 193−213.
12. Junker, M., and Creutz, C. E. (1994) Endonexin (annexin IV)-mediated lateral segregation of phosphatidylglycerol/phospatidylcholine membranes, *Biochemistry 33*, 8930−8940.
13. Rescher, U., Zobiack, N., and Gerke, V. (2000) Intact Ca(2+)-binding sites are required for targeting of annexin 1 to endosomal membranes in living HeLa cells, *J. Cell Sci. 113*, 3931−3938.
14. Isas, J. M., Patel, D. R., Jao, C., Jayasinghe, J., Cartailler, J.-P., Haigler, H. T., and Langen, R. (2003) Global structural changes in annexin 12, *J. Biol. Chem. 278*, 30227−30234.
15. Isas, J. M., Cartailler, J.-P., Sokolov, Y., Patel, D. R., Langen, R., Luecke, H., Hall, J. E., and Haigler, H. T. (2000) Annexins V and XII insert into bilayers at mildly acidic pH and form ion channels, *Biochemistry 39*, 3015−3022.
16. Concha, N. O., Head, J. F., Kaetzel, M. A., Dedman, J. R., and Seaton, B. A. (1993) Rat annexin V crystal structure: Ca(2+)-induced conformational changes, *Science 261*, 1321−1324.
17. Jin, M., Smith, C., Hsieh, H.-Y., Gibson, D. F., and Tait, J. F. (2004) Essential role of B-helix calcium binding sites in annexin V-membrane binding, *J. Biol. Chem. 279*, 40351−40357.
18. Dill, K. A., and Bromberg, S. (2003) *Molecular driving forces: statistical thermodynamics in chemistry and biology*, 1st ed., Garland Science, New York.
19. Babiychuk, E. B., and Draeger, A. (2000) Annexins in cell membrane dynamics: Ca^{2+}-regulated association of lipid microdomain, *J. Cell Biol. 150*, 1113−1123.
20. Hill, T. L. (1985) *Cooperativity theory in biochemistry. Steady-state and equilibrium systems*, Springer-Verlag, New York.
21. Wyman, J., and Gill, S. J. (1990) *Binding and Linkage*, University Science Books, Mill Valley, CA.
22. Capila, I., Hernaiz, M. J., Mo, Y. D., Mealy, T. R., Campos, B., Dedman, J. R., Linhardt, R. J., and Seaton, B. A. (2001) Annexin V−heparin oligosaccharide complex suggests heparan sulfate-mediated assembly on cell surfaces, *Structure 9*, 57−64.
23. Hinderliter, A., Biltonen, R. L., and Almeida, P. F. F. (2004) Lipid modulation of protein-induced membrane domains as a mechanism for control of signal transduction, *Biochemistry 43*, 7102−7110.
24. Hinderliter, A., Almeida, P. F. F., Creutz, C. E., and Biltonen, R. L. (2001) Domain formation in a fluid mixed lipid bilayer modulated through binding of the C2 protein motif, *Biochemistry 40*, 4181−4191.
25. Frazier, A. A., Roller, C. R., Havelka, J. J., Hinderliter, A., and Cafiso, D. S. (2003) Membrane-bound orientation and position of the synaptotagmin C2A domain by site-directed spin-labeling, *Biochemistry 42*, 96−105.
26. Rufener, E., Frazier, A. A., Wieser, C. M., Hinderliter, A., and Cafiso, D. S. (2005) Membrane-bound orientation and position of the synaptotagmin C2B domain determined by site-directed spin labeling, *Biochemistry 44*, 18−28.
27. Nelson, M. R., and Creutz, C. E. (1995) Comparison of the expression of native and mutant bovine annexin IV in *Escherichia coli* using four different expression systems, *Protein Expression Purif. 6*, 132−140.
28. Sohma, H., Creutz, C. E., Saitoh, M., Sano, H., Kuroki, Y., Voelker, D. R., and Akino, T. (1999) Characterization of the Ca^{2+}-dependent binding of annexin IV to surfactant protein A, *Biochem. J. 341*, 203−209.
29. Folch, J., Lees, M., and Sloane Stanley, G. H. (1957) A simple method for the isolation and purification of total lipides from animal tissues, *J. Biol. Chem. 226*, 497−509.
30. Selvin, P. R. (2002) Principles and biophysical applications of lanthanide-based probes, *Annu. Rev. Biophys. Biomol. Struct. 31*, 275−302.
31. Borin, G., Ruzza, P., Rossi, M., Calderan, A., Marchiori, F., and Perrion, E. (1989) Conformation and ion binding properties of peptides related to calcium binding domain III of bovine brain calmodulin, *Biopolymers 28*, 353−369.
32. Martin, R. B., and Richardson, F. S. (1979) Lanthanides as probes for calcium in biological systems, *Q. Rev. Biophys. 12*, 181−209.
33. Sopkova, J., Vincent, M., Takahashi, M., Lewit-Bentley, A., and Gallay, J. (1998) Conformational flexibility of domain III of annexin V studied by fluorescence of tryptophan 187 and circular dichroism: the effect of pH, *Biochemistry 37*, 11962−11970.
34. Patel, D. R., Jao, C. C., Mailliard, W. S., Isas, J. M., Langen, R., and Haigler, H. T. (2001) Calcium-dependent binding of annexin 12 to phospholipid bilayers: stoichiometry and implications, *Biochemistry 40*, 7054−7060.
35. Press, W. H., Teukolsky, S. A., Vetterling, W. T., and Flannery, B. P. (1994) *Numerical Recipes in Fortran*, 2nd ed., Cambridge University Press, New York.
36. Hill, A. V. (1913) The combinations of haemoglobin with oxygen and with carbon monoxide, *Biochem. J. 7*, 471−480.
37. Sutton, B. R., and Sprang, S. R. (1996) *Annexins: molecular structure to cell function* (Seaton, B. A., Ed.) pp 31−42, Landes, Georgetown, TX.
38. Kaetzel, M. A., Mo, Y. D., Mealy, T. R., Campos, B., Bergsma-Schutter, W., Brisson, A., Dedman, J. R., and Seaton, B. A. (2001) Phosphorylation mutants elucidate the mechanism of annexin IV-mediated membrane aggregation, *Biochemistry 40*, 4192−4199.
39. Swairjo, M. A., Concha, N. O., Kaetzel, M. A., Dedman, J. R., and Seaton, B. A. (1995) Ca(2+)-bridging mechanism and phospholipid headgroup recognition in the membrane-binding protein annexin V, *Nat. Struct. Biol. 2*, 968−974.
40. Bewley, M. C., Boustead, C. M., Walker, J. H., Waller, D. A., and Huber, R. (1993) Structure of chicken annexin V at 2.25-Å resolution, *Biochemistry 32*, 3923−3929.
41. Sopkova, J., Renouard, M., and Lewit-Bentley, A. (1993) The crystal structure of a new high-calcium form of annexin V, *J. Mol. Biol. 234*, 816−825.
42. Burger, A., Voges, D., Demange, P., Perez, C. R., Huber, R., and Berendes, R. (1994) Structural and electrophysiological analysis of annexin V mutants. Mutagenesis of human annexin V, an in vitro voltage-gated calcium channel, provides information about the structural features of the ion pathway, the voltage sensor and the ion selectivity filter, *J. Mol. Biol. 237*, 479−499.
43. Huber, R., Berendes, R., Burger, A., Luecke, H., and Karshikov, A. (1992) Annexin V-crystal structure and its implications on function, *Behring Inst. Mitt. 91*, 107−125.
44. Mo, Y., Campos, B., Mealy, T. R., Commodore, L., Head, J. F., Dedman, J. R., and Seaton, B. A. (2003) Interfacial basic cluster

in annexin V couples phospholipid binding and trimer formation on membrane surfaces, *J. Biol. Chem. 278*, 2437−2443.
45. Cutsforth, G. A., Whitaker, R. N., Hermans, J., and Lentz, B. R. (1989) A new model to describe extrinsic protein binding to phospholipid membranes of varying composition: application to human coagulation proteins, *Biochemistry 28*, 7453−7459.
46. Lentz, B. R., and Hermans, J. (1989) A new model to describe extrinsic protein binding to phospholipid membranes of varying composition: quantitative development, *Biochemistry 28*, 7459−7461.
47. Drust, D. S., and Creutz, C. E. (1988) Aggregation of chromaffin granules by calpactin at micromolar levels of calcium, *Nature 331*, 88−91.
48. Rosengarth, A., Gerke, V., and Lueke, H. (2001) X-ray structure of full-length annexin 1 and implications for membrane aggregation, *J. Mol. Biol. 306*, 489−498.
49. Favier-Peron, B., Lewit-Bentley, A., and Russo-Marie, F. (1996) The high-resolution crystal structure of human annexin III shows subtle differences with annexin V, *Biochemistry 35*, 1740−1744.
50. Hofmann, A., Raguenes-Nicol, C., Favier-Perron, B., Mesonero, J., Huber, R., Russo-Marie, F., and Lewit-Bentley, A. (2000) The annexin a3-membrane interaction is modulated by an N-terminal tryptophan, *Biochemistry 39*, 7712−7721.
51. Turnay, J., Olmo, N., Gasset, M., IIoro, I., Arrondo, J. L. R., and Lizarbe, M. A. (2002) Calcium-dependent conformational rearrangements and protein stability in chicken annexin a5, *Biophys. J. 83*, 2280−2291.
52. Arboledas, D., Olmo, N., Lizarbe, M. A., and Turnay, J. (1997) Role of the N-terminus in the structure and stability of chicken annexin V, *FEBS Lett. 416*, 217−220.
53. Vogl, T., Jatzke, C., Hinz, H.-J., Benz, J., and Huber, R. (1997) Thermodynamic stability of annexin V E17G: equilibrium parameters from an irreversible unfolding reaction, *Biochemistry 36*, 1657−1668.
54. Rosengarth, A., Rösgen, J., Hinz, H.-J., and Gerke, V. (1999) A comparison of the energetics of annexin I and annexin V, *J. Mol. Biol. 288*, 1013−1025.
55. Isas, J. M., Langen, R., Hubbell, W. L., and Haigler, H. T. (2004) Structure and dynamics of a helical hairpin that mediates calcium-dependent membrane binding of annexin B12, *J. Biol. Chem. 279*, 32492−32498.

BI050474G